THE JOURNAL OF NAVIGATION (2018), **71**, 1161–1177.
doi:10.1017/S0373463318000140

A Low Complexity Integrated Navigation System for Underwater Vehicles

Mehdi Emami[1] and Mohammad Reza Taban[2]

[1](*Department of Electrical Engineering, Yazd University, Yazd, Iran*)
[2](*Department of Electrical and Computer Engineering, Isfahan University of Technology, Isfahan 84156-83111, Iran*)
(E-mail: mrtaban@cc.iut.ac.ir)

This paper proposes a simplified algorithm for reducing the computational load of the conventional underwater integrated navigation system. The system usually comprises a three-dimensional accelerometer, a three-dimensional gyroscope, a three-dimensional Doppler Velocity Log (DVL) and a data fusion algorithm, such as a Kalman Filter (KF). Since the expected variations of roll, pitch and depth are small, these quantities are assumed to be constant, and the proposed system is designed in a two-dimensional form. Due to the low speed of the vehicle, the nonlinear dynamic equation of the velocity can be simplified in a linear form. We also simplify the conventional KF in order to avoid matrix multiplications and matrix inversions. The performance of the designed system is evaluated in a sea trial by an Autonomous Underwater Vehicle (AUV). The results show that the proposed system can significantly reduce the computational load of the conventional integrated navigation system without a significant reduction in position and velocity accuracy.

KEYWORDS

1. DVL. 2. Integrated navigation system. 3. Kalman filter.
4. Inertial Navigation System (INS). 5. Computational burden.

Submitted: 19 November 2016. Accepted: 28 February 2018. First published online: 9 May 2018.

1. INTRODUCTION. Accurate positioning of surface and airborne vehicles such as ships and airplanes is possible using Global Navigation Satellite Systems (GNSS) such as the Global Positioning System (GPS) (Grenon et al., 2001). However, since GPS signals do not penetrate beneath the water, this system cannot be used in underwater vehicles (Yun et al., 1999; Vasilijevic et al., 2012). For this reason, Inertial Navigation Systems (INS) are utilised as an alternative solution in many underwater applications (Titterton and Weston, 2004). The INS computes attitude, velocity and position of the vehicle using an Inertial Measurement Unit (IMU) which consists of three orthogonal accelerometers and three orthogonal gyroscopes (Xian et al., 2014; Kaygisiz and Sen, 2015; Wang et al., 2016).

In order to reduce the accumulative error of an INS, some auxiliary sensors are normally used (Shabani et al., 2013). In underwater applications, a Doppler Velocity Log (DVL) is usually utilised as an auxiliary sensor (Kinsey et al., 2006; Farrell, 2008). Incorporation of INS information with DVL measurements plays an important role in limiting INS errors (Shabani and Gholami, 2016). In underwater integrated navigation systems, a Kalman Filter (KF) is the conventional approach for data incorporation. This algorithm is a powerful and effective approach for incorporating noisy measurements of multiple sensors used for estimating the state of a time-varying system (Grewal et al., 2007). To date, numerous studies have utilised the KF for incorporating a DVL with an INS DVL (McEwen et al., 2005; Lee et al., 2007; Miller et al., 2010; Hegrenaes and Hallingstad, 2011; Shabani et al., 2015; Gao et al., 2015). Although the development of processor technology enables the implementation of KF-based INS/DVL integration, a reduction of computation load can facilitate the selection of processor type and thereby, reduce costs.

In most AUVs and embedded systems, like decoys (deceptive AUVs designed to counter torpedoes) and some oceanographic AUVs, simplicity is one of the most important aspects in designing and implementing processing algorithms. For example, the conventional KF algorithm has not been wildly used in such embedded systems due to its intrinsic computational complexity (Valade et al., 2017).

There are many features that can restrict the designer in choosing the processor type. Simplifying the algorithm can overcome some of the limitations such as performance (Floating Point Operations Per Second - FLOPS), power consumption and heat loss. In this paper, the KF equations used in navigation have been simplified such that the navigation algorithm can be implemented on a simple microcontroller.

In conventional INS/DVL systems, three mutually orthogonal accelerometers, three mutually orthogonal gyroscopes and a Three-Dimensional (3D) DVL are utilised. In practice, fewer sensors may be used depending on the type of vehicle used and the missions defined for it (Brandt and Gardner, 1996; Iqbal et al., 2009; Georgy et al., 2010). Underwater vehicles usually move with only small roll and pitch motions, and the vehicle's depth is measured through a pressure sensor. In addition, the sensitivity of navigation equations with respect to depth variation is very low. Therefore, in this work, the roll and pitch quantities were withdrawn from the navigation equations. In the proposed system, a two-axis accelerometer, a single-axis gyroscope, and a two-dimensional DVL have been utilised. Although the Coriolis effect makes the velocity equation nonlinear, in this work, this effect has been ignored because the discussed vehicles have low speed. This allows the velocity equation to be linearized; hence, it is not necessary to calculate Jacobian matrices.

Recently, the computational burden of integrated navigation systems has decreased through reducing the number of inertial sensors and simplifying the INS equations. For instance, Brandt and Gardner (1996) reduced the number of inertial sensors required for navigating a land vehicle by defining some constraints on vehicle motion. In their system, a single-axis accelerometer, a three-axis gyroscope and an odometer were used for estimating the vehicle's speed. Iqbal et al. (2008) proposed a low-cost navigation system for land vehicles including a single-axis gyroscope and a two-axis accelerometer accompanying a GPS receiver and an odometer. Hoshizaki and Tashiro (2009) decreased the computational burden of a Micro-Electromechanical System (MEMS) INS by considering the Earth to be flat and ignoring the Earth's rotation and the rotation of the local tangent plane with respect to the Earth. Moreover, they assumed the pitch and roll angles of vehicles to be less than 90°. Zhang et al. (2013) proposed a simplified INS/GPS algorithm where the Coriolis

https://doi.org/10.1017/S0373463318000140 Published online by Cambridge University Press

acceleration in the velocity equation and rotation correction were disregarded. Furthermore, the sampling frequency of inertial sensors and the number of system states were reduced.

Another way to simplify an INS is to reduce the complexity of the KF algorithm. In a conventional KF, compared to a fully integrated navigation system, matrix multiplications and matrix inversions are executed. In this paper, by using some assumptions, the KF equations have been simplified such that the computational burden has been significantly decreased compared with the conventional algorithm.

In order to assess the proposed system, a sea test was conducted using an Autonomous Underwater Vehicle (AUV). Experimental results illustrate that despite a considerable reduction of computational load, the accuracy of the proposed system does not noticeably decrease compared with that of a more conventional system. The structure of the paper is as follows. In Section 2, the conventional INS/DVL integrated navigation system is reviewed. In Section 3, the proposed algorithm will be presented. The results of the experimental test are presented in Section 4. Finally, the paper is concluded in Section 5.

2. CONVENTIONAL INTEGRATED NAVIGATION SYSTEM.

In this section, first, the dynamic equations of the system and measurement for the INS/DVL integrated navigation system are introduced. Then, we review the KF equations based on our model.

2.1. *System dynamic equations.*

The total state vector of the system includes position, velocity and orientation (roll, pitch and heading) vectors. In general, the dynamic equations of the navigation system are nonlinear. The general form of the continuous-time nonlinear state-space model is defined by (Simon, 2006):

$$\dot{\mathbf{x}} = \mathbf{f}(\mathbf{x}, \mathbf{u}, \mathbf{w}) \tag{1}$$

where $\mathbf{x} = \left[(\mathbf{p}^{\boldsymbol{n}})^T \quad (\mathbf{v}^{\boldsymbol{n}})^T \quad (\boldsymbol{\zeta})^T\right]^T$ is the system state vector; $\mathbf{p}^{\boldsymbol{n}} = \left[L \quad l \quad d\right]^T$, $\mathbf{v}^{\boldsymbol{n}} = \left[v_N \quad v_E \quad v_D\right]^T$ and $\boldsymbol{\zeta} = \left[\phi \quad \theta \quad \psi\right]^T$ are position, velocity and orientation vectors; L, l and d are latitude, longitude and depth; v_N, v_E and v_D are velocity components in the north, east and down directions and ϕ, θ and ψ are roll, pitch and heading angles, respectively. $\mathbf{u}$ is the control input vector and is given as $\mathbf{u} = \left[\left(\mathbf{f}^b\right)^T \quad \left(\boldsymbol{\omega}_{ib}^b\right)^T\right]^T$ where $\mathbf{f}^b = \left[f_x \quad f_y \quad f_z\right]^T$ is the vehicle's specific force vector with respect to the inertial frame resolved in the body frame and $\boldsymbol{\omega}_{ib}^b = \left[\omega_x \quad \omega_y \quad \omega_z\right]^T$ is the vehicle's angular rate relative to the inertial frame represented in the body frame. $\mathbf{w}$ is the process noise caused by uncertainty in $\mathbf{u}$. The process noise contains a fixed (or slowly time-varying) bias and a zero-mean white noise. Bias of the sensors can be estimated before movement of the AUV by the method stated in Farrell (2008). In other words, the bias in navigation equations can be assumed to be definite and omitted after receiving the measurements of the accelerometer and gyroscope. So, $\mathbf{w}$ can be defined as:

$$\mathbf{w} = \left[\mathbf{w}_a^T \quad \mathbf{w}_g^T\right]^T \tag{2}$$

where $\mathbf{w}_a = \left[w_{ax} \quad w_{ay} \quad w_{az}\right]^T$ and $\mathbf{w}_g = \left[w_{gx} \quad w_{gy} \quad w_{gz}\right]^T$ are zero mean white noise components of the accelerometer and gyroscope measurements. Hence $\mathbf{w}$ is a 6x1 vector with Power Spectral Density (PSD) matrix $\mathbf{Q}_c$ which is formed as a diagonal

https://doi.org/10.1017/S0373463318000140 Published online by Cambridge University Press

matrix:

$$\mathbf{Q}_c = \begin{bmatrix} \sigma_a^2 \mathbf{I}_3 & \mathbf{0}_3 \\ \mathbf{0}_3 & \sigma_g^2 \mathbf{I}_3 \end{bmatrix} \tag{3}$$

where σ_a and σ_g are the standard deviations of the accelerometer and gyroscope noises, respectively. $\mathbf{I}_3$ and $\mathbf{0}_3$ are two 3×3 identity and zero matrices, respectively. The dynamic equation of state space, $\mathbf{f}$, is a nonlinear vector function and is given as (Titterton and Weston, 2004):

$$\mathbf{f}(\mathbf{x}, \mathbf{u}, \mathbf{w}) = \begin{bmatrix} \boldsymbol{\Gamma} \mathbf{v}^{\mathbf{n}} \\ \mathbf{C}_b^{\mathbf{n}} \left(\mathbf{f}^b + \mathbf{w}_a \right) - \left(2\boldsymbol{\omega}_{ie}^n + \boldsymbol{\omega}_{en}^n \right) \times \mathbf{v}^n + \mathbf{g}^n \\ \mathbf{A}^{-1} \boldsymbol{\omega}_{nb}^b \end{bmatrix} \tag{4}$$

where

$$\boldsymbol{\Gamma} = \begin{bmatrix} \dfrac{1}{R_N + d} & 0 & 0 \\ 0 & \dfrac{secL}{R_E + d} & 0 \\ 0 & 0 & 1 \end{bmatrix} \tag{5}$$

$$\mathbf{A} = \begin{bmatrix} 1 & 0 & -sin\theta \\ 0 & cos\phi & sin\phi cos\theta \\ 0 & sin\phi & cos\phi cos\theta \end{bmatrix} \tag{6}$$

$$\boldsymbol{\omega}_{nb}^b = \boldsymbol{\omega}_{ib}^b + \mathbf{w}_g - \boldsymbol{\omega}_{in}^b \tag{7}$$

$$\boldsymbol{\omega}_{ie}^n = \begin{bmatrix} \Omega cosL & 0 & -sinL \end{bmatrix}^{\boldsymbol{T}} \tag{8}$$

$$\boldsymbol{\omega}_{en}^n = \begin{bmatrix} \dfrac{v_E}{R_E + d} & -\dfrac{v_N}{R_N + d} & -\dfrac{v_E}{R_E + d} tanL \end{bmatrix}^{\boldsymbol{T}} \tag{9}$$

$$R_N = \frac{R(1 - e^2)}{(1 - e^2 sin^2 L_k)^{1 \cdot 5}}, R_E = \frac{R}{(1 - e^2 sin^2 L_k)^{0 \cdot 5}} \tag{10}$$

where $R = 6378137m$, $e = 0{\cdot}0818191908425$ and $\Omega = 7{\cdot}292115 \times 10^{-5}$ rad/s are the length of the semi major axis of the Earth, the major eccentricity of the ellipsoid of the Earth, and the Earth angular rate, respectively. $\mathbf{C}_b^{\mathbf{n}}$ is the transformation matrix from the body frame to the navigation frame as:

$$\mathbf{C}_b^{\boldsymbol{n}} = \begin{bmatrix} cos\theta cos\psi & -cos\phi sin\psi + sin\phi sin\theta cos\psi & sin\phi sin\psi + cos\phi sin\theta cos\psi \\ cos\theta sin\psi & cos\phi cos\psi + sin\phi sin\theta sin\psi & -sin\phi cos\psi + cos\phi sin\theta sin\psi \\ -sin\theta & sin\phi cos\theta & cos\phi cos\theta \end{bmatrix} \tag{11}$$

Moreover, $\mathbf{g}^n = \begin{bmatrix} 0 & 0 & g \end{bmatrix}^T$ is the gravity vector represented in the navigation frame, and g is defined by:

$$g = \frac{g_0}{\left(1 + \dfrac{d}{R_0} \right)^2} \tag{12}$$

https://doi.org/10.1017/S0373463318000140 Published online by Cambridge University Press

$$g_0 = 9{\cdot}780318 \times (1 + 5{\cdot}3024 \times 10^{-3} sin^2 L - 5{\cdot}9 \times 10^{-6} sin^2 2L)$$

$$R_0 = \sqrt{R_N R_E}$$

where L and R_0 are the latitude and the mean radius of curvature.

2.2. *Measurement equations.* In the proposed system, the measurements of the DVL are considered as auxiliary signals which have a nonlinear relationship with the system states. The measurement model may be expressed as follows:

$$\mathbf{v}^b = \mathbf{h}(\mathbf{x}) + \boldsymbol{\upsilon}_{\boldsymbol{v}} = \left(\mathbf{C}_b^{\boldsymbol{n}}\right)^{-1} \mathbf{v}^n + \boldsymbol{\upsilon}_{\boldsymbol{v}} \tag{13}$$

where $\mathbf{v}^b = \begin{bmatrix} v_x & v_y & v_z \end{bmatrix}^T$ is the measurement vector of the DVL represented in the body frame and $\boldsymbol{\upsilon}_{\boldsymbol{v}} = \begin{bmatrix} \upsilon_x & \upsilon_y & \upsilon_z \end{bmatrix}^T$ is the noise vector of the DVL measurements which is modelled as a white noise vector with zero mean and covariance matrix $\mathbf{R}$ as:

$$\mathbf{R} = \begin{bmatrix} \sigma_{\upsilon_x}^2 & 0 & 0 \\ 0 & \sigma_{\upsilon_y}^2 & 0 \\ 0 & 0 & \sigma_{\upsilon_z}^2 \end{bmatrix} \tag{14}$$

where $\sigma_{\upsilon_x}^2$, $\sigma_{\upsilon_y}^2$ and $\sigma_{\upsilon_z}^2$ are the variances of the DVL measurements.

2.3. *Data integration.* It is not possible to use a linear KF in an INS/DVL integrated navigation, since the navigation equation are non-linear. In such cases, the Extended Kalman Filter (EKF) is utilised for data incorporation. The EKF functions in two stages, the prediction and correction steps, which are described in the following sections. We have considered the system in discrete time form in which k denotes the present time t_k.

2.3.1. *Prediction step.* In the prediction procedure, the system state is predicted as (Sarkka, 2013):

$$\hat{\mathbf{x}}_k^- = \int_{t_{k-1}}^{t_k} \mathbf{f}\left(\hat{\mathbf{x}}_{k-1}^+, \mathbf{u}_{k-1}, 0\right) dt \tag{15}$$

$$\mathbf{P}_k^- = \mathbf{A}_{k-1} \mathbf{P}_{k-1}^+ \mathbf{A}_{k-1}^T + \mathbf{Q}_{k-1} \tag{16}$$

where $\hat{\mathbf{x}}_k^-$ and $\hat{\mathbf{x}}_k^+$ are the state estimates in prediction and correction steps; $\mathbf{P}_k^-$ and $\mathbf{P}_k^+$ are the covariance matrices of state estimates in prediction and correction steps, respectively, and dt is the sampling time of the inertial sensors. Discretised matrices $\mathbf{A}_k$ and $\mathbf{Q}_k$ at time t_k are computed as (Maybeck, 1979):

$$\mathbf{A}_k = e^{(\mathbf{F}_k . dt)} \approx \mathbf{I} + \mathbf{F}_k dt \tag{17}$$

$$\mathbf{Q}_k \approx \mathbf{G}_k \mathbf{Q}_k \mathbf{G}_k^T dt^2 \tag{18}$$

where Jacobian matrices $\mathbf{F}_k$ and $\mathbf{G}_k$ are computed as follows:

$$\mathbf{F}_k = \left[\frac{\partial \mathbf{f}}{\partial \mathbf{x}}\right]_{\hat{\mathbf{x}}_k^-}, \mathbf{G}_k = \left[\frac{\partial \mathbf{f}}{\partial \mathbf{w}}\right]_{\hat{\mathbf{x}}_k^-} \tag{19}$$

https://doi.org/10.1017/S0373463318000140 Published online by Cambridge University Press

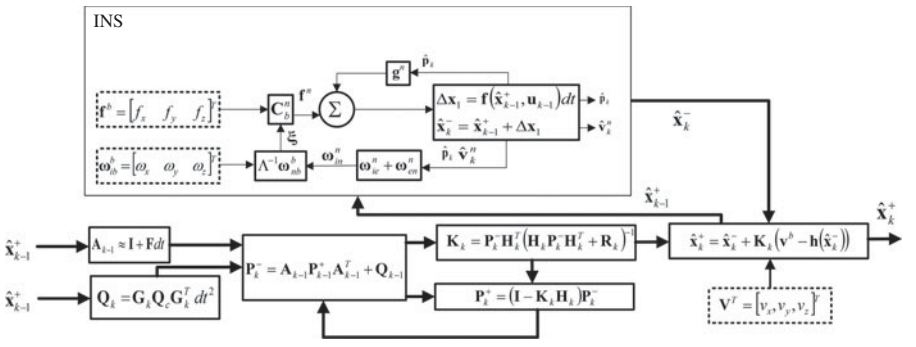

Figure 1. The conventional INS/DVL integrated navigation system. The upper box named INS represents the dynamic system (Equations (1)–(12)) and the other blocks represent data integration and the correction step (Equations (13)–(25)).

The prediction Equation (15) can easily be approximated as the follows:

$$\hat{\mathbf{x}}_k^- = \hat{\mathbf{x}}_{k-1}^+ + \Delta\mathbf{x}_1 \tag{20}$$

$$\Delta\mathbf{x}_1 = \mathbf{f}\left(\hat{\mathbf{x}}_{k-1}^+, \mathbf{u}_{k-1}, 0\right) dt \tag{21}$$

2.3.2. *Correction Step.* By receiving new auxiliary data from the DVL, the navigation state and its covariance matrix at time t_k are corrected by the following equations (Sarkka, 2013):

$$\mathbf{K}_k = \mathbf{P}_k^- \mathbf{H}_k^T \left(\mathbf{H}_k \mathbf{P}_k^- \mathbf{H}_k^T + \mathbf{R}\right)^{-1} \tag{22}$$

$$\hat{\mathbf{x}}_k^+ = \hat{\mathbf{x}}_k^- + \mathbf{K}_k \left(\mathbf{v}^b - \mathbf{h}\left(\hat{\mathbf{x}}_k^-\right)\right) \tag{23}$$

$$\mathbf{P}_k^+ = \left(\mathbf{I} - \mathbf{K}_k \mathbf{H}_k\right) \mathbf{P}_k^- \tag{24}$$

where $\mathbf{K}_k$ is the Kalman gain; $\mathbf{I}$ is the identity matrix; and measurement output matrix $\mathbf{H}_k$ is computed through linearizing Equation (13) as:

$$\mathbf{H}_k = \left.\frac{\partial\left(\left(\mathbf{C}_b^{\mathbf{n}}\right)^{-1}\mathbf{v}^n\right)}{\partial\mathbf{x}}\right|_{\hat{\mathbf{x}}_k^-} \tag{25}$$

The block diagram of the conventional INS/DVL integrated navigation system is illustrated in Figure 1.

3. PROPOSED INTEGRATED NAVIGATION SYSTEM. In underwater vehicles, depth may be measured by a pressure sensor. In addition, in cruise conditions, the vehicle maintains a state of equilibrium, that is the vehicle's roll and pitch are small. Furthermore, the vertical component of the vehicle's velocity is usually small. This means that, in the proposed system, the required computations might be reduced to Two-Dimensional (2D)

https://doi.org/10.1017/S0373463318000140 Published online by Cambridge University Press

space. Hence, the transformation matrix $\mathbf{C}_b^n$ would change to

$$\mathbf{C}_b^{\mathbf{n}} = \begin{bmatrix} cos\psi & -sin\psi \\ sin\psi & cos\psi \end{bmatrix} \tag{26}$$

In the proposed system, the state vector contains vehicle velocities in the north and east directions as $\mathbf{v}^n = \begin{bmatrix} v_N & v_E \end{bmatrix}^T$, and the velocity measured by DVL $\mathbf{v}^b = \begin{bmatrix} v_x & v_y \end{bmatrix}^T$ is considered as an auxiliary measurement. After estimating the state vector, latitude and longitude are calculated through a Dead Reckoning (DR) algorithm. Assuming the vehicle has low velocity, the Coriolis effect $\left(2\boldsymbol{\omega}_{ie}^n + \boldsymbol{\omega}_{en}^n\right) \times \mathbf{v}^n$ is always small and may be ignored and then the velocity equation can be rewritten as follows:

$$\dot{\mathbf{v}}^n = \mathbf{C}_b^n \mathbf{f}^b + \mathbf{C}_b^n \mathbf{w}_a, \mathbf{f}^b = \begin{bmatrix} f_{\mathbf{x}} & f_{\mathbf{y}} \end{bmatrix}^T \tag{27}$$

In the proposed system, the matrices $\mathbf{F}_k$, $\mathbf{A}_k$ and $\mathbf{G}_k$, and are obtained from Equation (27) as follows:

$$\mathbf{F}_k = \mathbf{0}, \mathbf{A}_k = \mathbf{I}, \mathbf{G}_k = \mathbf{C}_b^n \tag{28}$$

where $\mathbf{I}$ and $\mathbf{0}$ are 2×2 identity and zero matrices. By assuming similar and independent accelerometers, $\mathbf{Q}_k$ is computed as follows:

$$\mathbf{Q}_k \approx \mathbf{C}_b^n \mathbf{Q}_c \left(\mathbf{C}_b^n\right)^T dt^2 = \sigma_a^2 \mathbf{I} dt^2 \tag{29}$$

which shows that $\mathbf{Q}_k$ is a diagonal matrix with the same elements at all time steps. Matrix $\mathbf{H}$ is computed from Equation (25) as follows:

$$\mathbf{H} = \left(\mathbf{C}_b^n\right)^{-1} \tag{30}$$

By assuming DVL measurements have independent and identically distributed noise in x and y directions, Equation (16) may be rewritten according to Equations (22) and (24) as:

$$\mathbf{P}_k^- = \mathbf{P}_{k-1}^- - \mathbf{P}_{k-1}^- \mathbf{H}_{k-1}^T \left(\mathbf{H}_{k-1} \mathbf{P}_{k-1}^- \mathbf{H}_{k-1}^T + \sigma_v^2 \mathbf{I}\right)^{-1} \mathbf{H}_{k-1} \mathbf{P}_{k-1}^- + \sigma_a^2 \mathbf{I} dt^2 \tag{31}$$

Since $\mathbf{H}_k \mathbf{H}_k^T = \mathbf{I}$ and $\mathbf{P}_k^-$ is assumed to be a zero matrix at $k = 0$, $\mathbf{P}_k^-$ at $k = 1$ is given by the equation:

$$\mathbf{P}_1^- = \sigma_a^2 \mathbf{I} dt^2 = P_1 \mathbf{I} \tag{32}$$

In other words, $\mathbf{P}_1^-$ is a diagonal matrix with equal elements. Similarly, according to Equations (29) and (32), $\mathbf{P}_2^-$ may be given as follows:

$$\begin{aligned} \mathbf{P}_2^- &= P_1 \mathbf{I} - P_1 \mathbf{H}_1^T \left(P_1 \mathbf{H}_1 \mathbf{H}_1^T \mathbf{I} + \sigma_v^2 \mathbf{I}\right)^{-1} \mathbf{H}_1 P_1 \mathbf{I} + \sigma_a^2 \mathbf{I} dt^2 \\ &= P_1 \mathbf{I} - \frac{P_1^2}{P_1 + \sigma_v^2} \mathbf{I} + \sigma_a^2 \mathbf{I} dt^2 = P_2 \mathbf{I} \end{aligned} \tag{33}$$

The above equation shows that $\mathbf{P}_2^-$ is also a diagonal matrix with equal elements. By generalising the above procedure, it can easily be shown that $\mathbf{P}_k^-$ is a diagonal matrix with the

https://doi.org/10.1017/S0373463318000140 Published online by Cambridge University Press

same elements at all time steps as $\mathbf{P}_k^- = P_k\mathbf{I}$. Generally, Equation (31) can be rewritten as:

$$\begin{aligned}\mathbf{P}_k^- &= P_{k-1}\mathbf{I} - P_{k-1}\mathbf{H}_{k-1}^T\left(P_{k-1}\mathbf{H}_{k-1}\mathbf{H}_{k-1}^T\mathbf{I} + \sigma_v^2\mathbf{I}\right)^{-1}\mathbf{H}_{k-1}P_{k-1}\mathbf{I} + \sigma_a^2\mathbf{I}dt^2 \\ &= \left(\frac{\sigma_v^2 P_{\mathrm{k}-1}}{P_{\mathrm{k}-1}+\sigma_v^2} + \sigma_a^2 dt^2\right)\mathbf{I} = \begin{bmatrix} P_{\mathrm{k}} & 0 \\ 0 & P_{\mathrm{k}} \end{bmatrix} = P_k\mathbf{I}\end{aligned} \tag{34}$$

Although the model of the navigation problem is a time-varying model, it is possible to prove by mathematical induction that P_{k} in Equation (34) is an asymptotic ascendant function which becomes equal to the constant value P:

$$P = \frac{\sigma_a^2 dt^2 + \sqrt{\left(\sigma_a^2 dt^2\right)^2 + 4\sigma_v^2\sigma_a^2 dt^2}}{2} \tag{35}$$

If the vehicle is kept motionless for long enough before starting navigation, it can be assumed that P_{k} equates to P from the first step time of navigation. In other words, from the instant of starting navigation, the constant value P can be used instead of P_{k}. Therefore, Equation (22) may be changed to:

$$\mathbf{K}_k = \frac{P}{P+\sigma_v^2}\mathbf{C}_b^{\boldsymbol{n}} \tag{36}$$

According to Equation (27), $\hat{\mathbf{x}}_k^-$ is expressed as follows:

$$\hat{\mathbf{x}}_k^- = \hat{\mathbf{x}}_{k-1}^+ + \mathbf{C}_b^{\boldsymbol{n}}\mathbf{f}^b\,dt \tag{37}$$

Using Equations (30), (36) and (37), Equation (23) may be expressed as:

$$\begin{aligned}\hat{\mathbf{x}}_k^+ &= \hat{\mathbf{x}}_k^- + \frac{P}{P+\sigma_v^2}\mathbf{C}_b^{\boldsymbol{n}}\left(\mathbf{v}^b - \left(\mathbf{C}_b^{\boldsymbol{n}}\right)^{-1}\hat{\mathbf{x}}_k^-\right) \\ &= \frac{\sigma_v^2}{P+\sigma_v^2}\hat{\mathbf{x}}_{k-1}^+ + \mathbf{C}_b^{\mathbf{n}}\left[\frac{P}{P+\sigma_v^2}\mathbf{v}^b + \frac{\sigma_v^2 dt}{P+\sigma_v^2}\mathbf{f}^b\right] \\ &= A\hat{\mathbf{x}}_{k-1}^+ + \mathbf{C}_b^{\mathbf{n}}\left[B\mathbf{v}^b + C\mathbf{f}^b\right]\end{aligned} \tag{38}$$

The scalar coefficients A, B and C in Equation (38) can be computed off-line and it is not necessary to recalculate them during system operation.

After estimating the velocity components in the north and east directions, the latitude and longitude are computed by the following equations:

$$L_k = L_{k-1} + dt\frac{v_N}{R_N}, l_k = l_{k-1} + dt\frac{v_E sec L_{k-1}}{R_E} \tag{39}$$

In Equation (38), $\mathbf{C}_b^{\boldsymbol{n}}$ must be computed at each iteration. However, calculation of sine and cosine functions is not required for this purpose. The reason is that these functions may be expressed as follows:

$$\begin{cases}\dfrac{d\,(sin\psi)}{dt} = \dot{\psi}\,cos\psi \\ \dfrac{d\,(cos\psi)}{dt} = -\dot{\psi}\,sin\psi\end{cases} \xrightarrow{\dot{\psi}=\omega_{z,k}} \begin{aligned}(sin\psi)_k &= (sin\psi)_{k-1} + \omega_{z,k}\,dt\,(cos\psi)_k \\ (cos\psi)_k &= (cos\psi)_{k-1} + \omega_{z,k}\,dt\,(sin\psi)_k\end{aligned} \tag{40}$$

where $\omega_{z,k}$ is the third component of the vehicle's angular velocity vector with respect to the navigation frame represented in the body frame $\boldsymbol{\omega}_{nb}^b$, and is calculated as follows in the

https://doi.org/10.1017/S0373463318000140 Published online by Cambridge University Press

Figure 2. The AUV used in the sea test.

proposed system:

$$\omega_{z,k} = r_k + \Omega sinL_k + v_{E,k}\frac{tanL_k}{R_E} \tag{41}$$

where r_k is the third component of the angular velocity vector $\boldsymbol{\omega}_{ib}^{b}$ at time step k. So, Equation (40) may be expressed as follows:

$$\begin{cases} C_{1,k} = (cos\psi)_k \\ C_{2,k} = (sin\psi)_k \end{cases} \xrightarrow{\dot{\psi}=\omega_{z,k}} \begin{array}{l} C_{1,k} = C_{1,(k-1)} + \omega_{z,k}dtC_{2,k} \\ C_{2,k} = C_{2,(k-1)} + \omega_{z,k}dtC_{1,k} \end{array} \tag{42}$$

Therefore, according to Equation (26), the transformation matrix at time step k is expressed as follows:

$$\mathbf{C}_{b,k}^{\boldsymbol{n}} = \begin{bmatrix} C_{1,k} & -C_{2,k} \\ C_{2,k} & C_{1,k} \end{bmatrix} \tag{43}$$

From Equation (42) we see that the value of $C_{2,k}$ has not yet been specified for computing $C_{1,k}$. To remedy this problem, the value $C_{2,(k-1)}$ has been used instead of $C_{2,k}$. Accordingly, by using Equation (26) instead of Equation (42), we can reduce the computational load through omitting the calculation of sine and cosine functions.

4. EXPERIMENTAL RESULTS. In this section, the performance of the proposed integrated navigation system is evaluated. For this purpose, a sea test was conducted using an AUV as shown in Figure 2. In this test, an Inertial Measurement Unit (IMU) and a DVL were utilised for navigation. A GPS and a high performance INS were used as the reference systems. In order to evaluate system accuracy, the position and velocity estimated by the proposed system are compared with those of a high performance INS/GPS/DVL integrated system. The technical specifications of the navigation and reference sensors are given in

https://doi.org/10.1017/S0373463318000140 Published online by Cambridge University Press

Table 1. Technical specifications of the main instruments.

ACCELEROMETER	
Bias	100 μg
Resolution	1 mg
Data Rate	20 Hz
GYROSCOPE	
Bias	0·01 *deg/hr*
Resolution	3·6 *deg/hr*
Data Rate	20 Hz
DVL	
Accuracy	1% $\pm$ 2 *mm/s* (1σ)
Data Rate	3 Hz

Table 2. Technical specifications of the reference instruments.

INS	
Position Accuracy	0·6 *NM/hr*
Data Rate	20 Hz
GPS	
Accuracy	$<$10 *m*
Data Rate	1 Hz
INS/GPS/DVL	
Position Accuracy	0·1% *of travelled distance*
Velocity Accuracy	0·1%
Data Rate	20 Hz

Tables 1 and 2, respectively. The trajectory travelled in the test is shown in Figure 3, in which the distance travelled and time are about 55·8 km and 4 hours, respectively.

According to the dynamic equations given in Section 2.1, the depth variable is added in addition to the radius of the Earth. As submarines and AUVs usually move in depths less than 500 m, the depth is small compared with the radius of the Earth and drawing out the depth from the equations has no effect on the position accuracy. Moreover, as shown in Figure 4 the maximum values of roll and pitch angles of the AUV are 2·03° and 0·9° respectively and fluctuate around zero. Therefore, eliminating them from the navigation equations has minimal effect on the position accuracy.

In Figures 5–7, the latitude, longitude and horizontal positions estimated by the proposed and conventional systems are shown. The position results imply that the accuracy of the proposed system is approximately equal to the conventional system. Note that the proposed method considerably reduces the computational burden.

In order to validate the estimated velocity, the horizontal velocity is utilised and the curves of the horizontal velocity measured by the DVL and estimated by the navigation algorithms are compared with each other. The horizontal velocity in Knots is computed as follows:

$$v_h = \sqrt{v_x^2 + v_y^2} \Big/ 0{\cdot}5144 \tag{44}$$

https://doi.org/10.1017/S0373463318000140 Published online by Cambridge University Press

Figure 3. Travelled trajectory in the sea test: In this test, approximately 55·8 km was travelled in 4 hours.

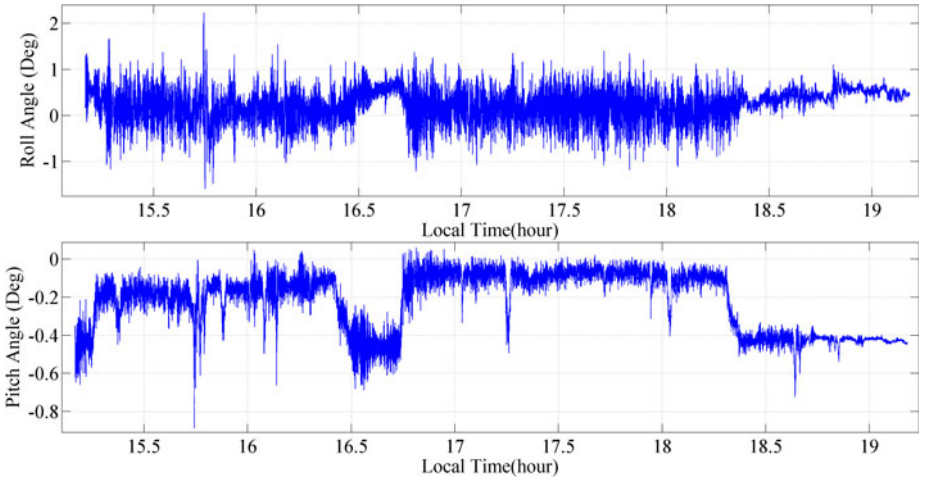

Figure 4. Changes of roll and pitch during the test.

where v_x and v_y in m/s are the velocity components in the x and y directions. In Figure 8, the curves of the horizontal velocity estimated by the proposed and conventional systems are shown compared with the reference system.

Although equations indicate that the Coriolis acceleration affects the speed of the AUV, the figures show that eliminating Coriolis acceleration does not have a great effect on the speed. This is due to the low speed of the AUV. The results of the estimated velocity also imply that the accuracy of the proposed system is identical to the conventional system.

https://doi.org/10.1017/S0373463318000140 Published online by Cambridge University Press

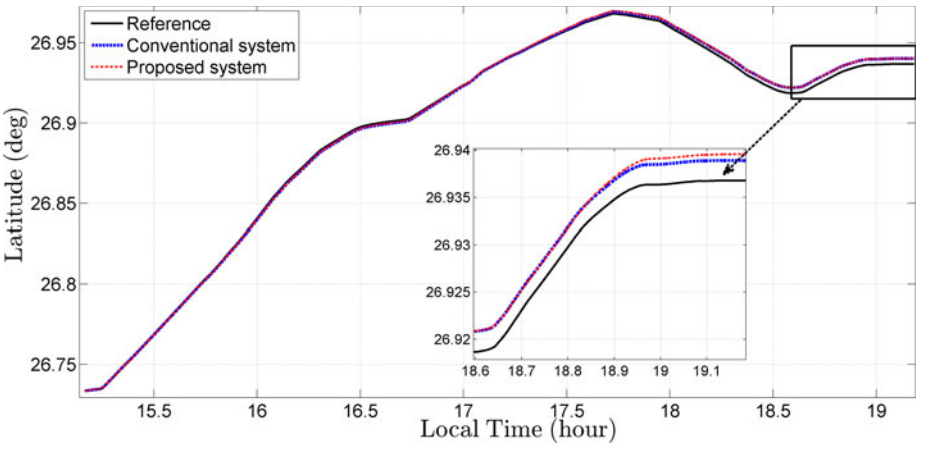

Figure 5. Comparison of latitudes estimated by proposed, conventional and reference systems.

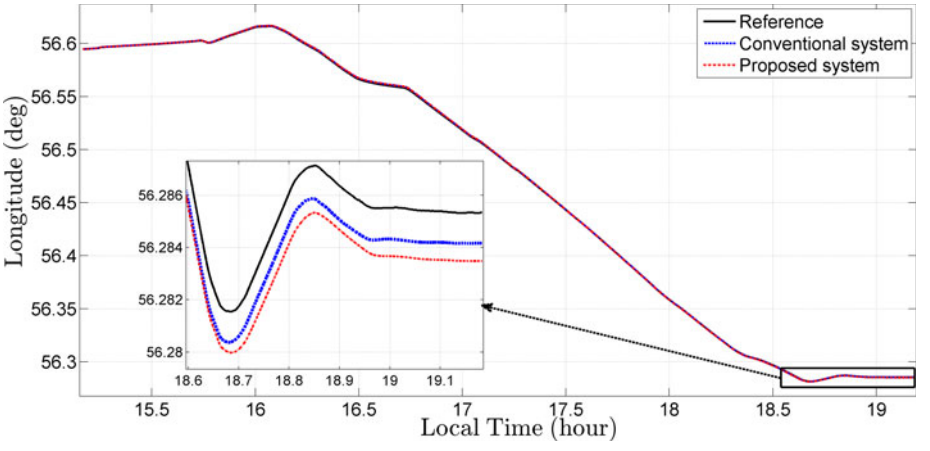

Figure 6. Comparison of longitudes estimated by proposed, conventional and reference systems.

In order to evaluate the performance of the proposed system, the measure of absolute error of the estimated position can be used. The absolute error at time step k is denoted by:

$$e_k = \left| \frac{R\left(L_{e,k} - L_{r,k}\right)}{cos\alpha_k} \right| \tag{45}$$

where $L_{e,k}$ and $L_{r,k}$ are the estimated and the reference latitudes at time step k, respectively, and angle α_k is obtained as follows (Forssell, 2008):

$$\alpha_k = arctan \frac{l_{e,k} - l_{r,k}}{ln\left(\dfrac{tan\left(\dfrac{L_{e,k}}{2} - \dfrac{\pi}{4}\right)}{tan\left(\dfrac{L_{r,k}}{2} - \dfrac{\pi}{4}\right)}\right)} \tag{46}$$

https://doi.org/10.1017/S0373463318000140 Published online by Cambridge University Press

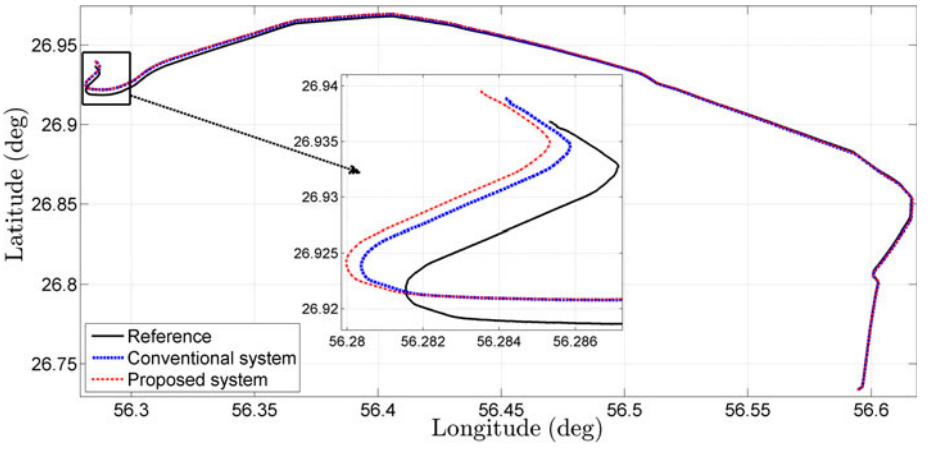

Figure 7. Comparison of horizontal positions estimated by proposed, conventional and reference systems.

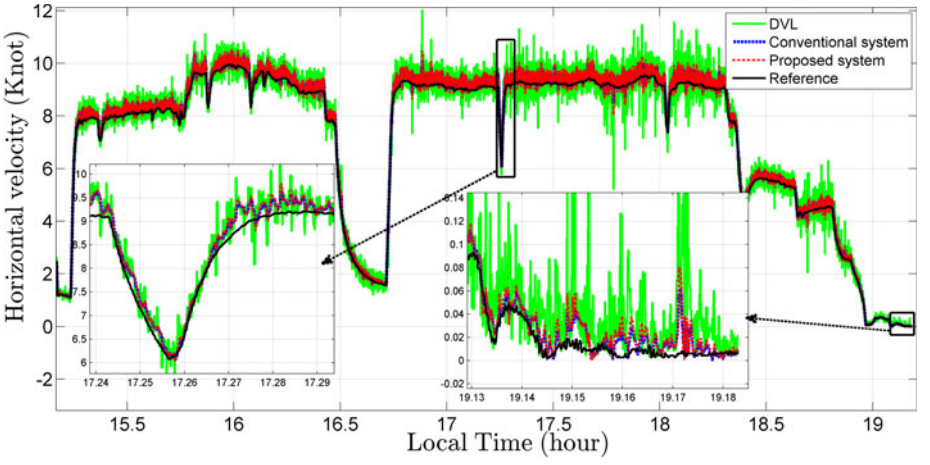

Figure 8. Comparison of horizontal velocity estimated by the proposed, conventional and reference systems.

where $l_{e,k}$ and $l_{r,k}$ are the estimated and reference longitudes at time step k respectively. In Figure 9, curves of the absolute error of estimated position corresponding to the proposed and conventional systems are compared. It can be seen that the performances are close together. In pure inertial mode, Equation (38) changes to:

$$\hat{\mathbf{x}}_k^+ = \hat{\mathbf{x}}_{k-1}^+ + \mathbf{C}_b^{\mathbf{n}} \mathbf{f}^b dt \tag{47}$$

In Figure 10, curves of the absolute error of the estimated position corresponding to the proposed and conventional systems in pure inertial mode are compared. Results show that, after about four hours, the proposed algorithm has increased the error to only 800 m, while the computational burden has significantly decreased compared with the conventional algorithm.

In order to quantitatively compare the proposed system with a more conventional system, Root Mean Square Error (RMSE) is used for position and velocity estimations defined

https://doi.org/10.1017/S0373463318000140 Published online by Cambridge University Press

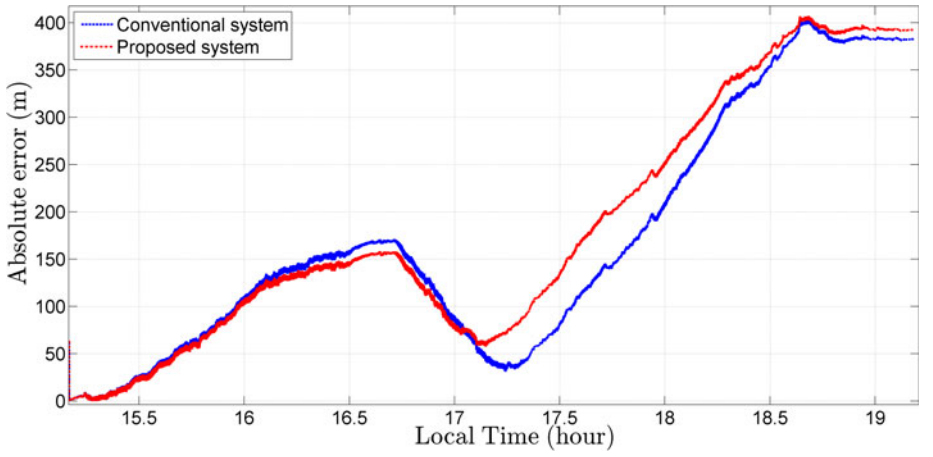

Figure 9. Comparison of the absolute error related to the position estimated by the proposed and conventional systems.

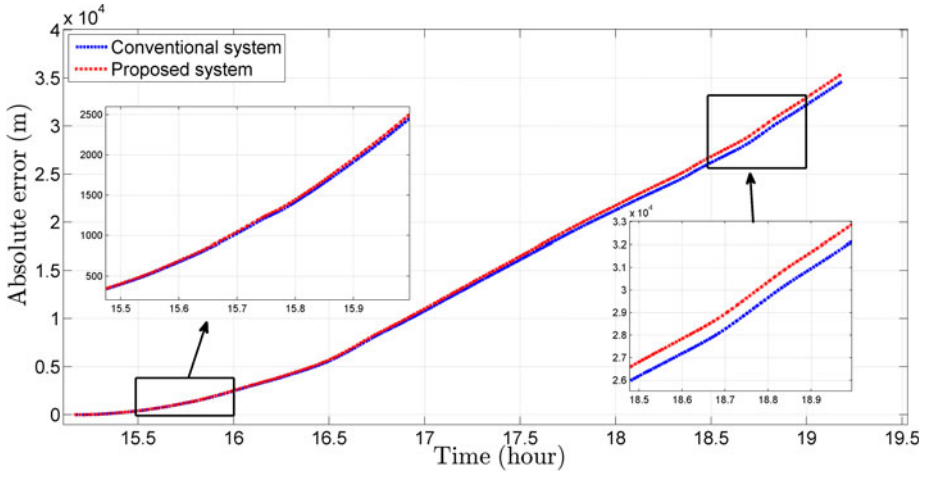

Figure 10. Comparison of the pure inertial absolute error related to the position estimated by the proposed and conventional systems.

by the following equations:

$$Position\ RMSE = sqrt\left(mean(e_k^2)\right) \tag{48}$$

$$Relative\ RMSE = \frac{RMSE}{Travelled\ Distance} \times 100 \tag{49}$$

$$Velocity\ RMSE = sqrt\left(mean\left(\left(v_{h,r} - v_{h,e}\right)^2\right)\right) \tag{50}$$

where $v_{h,r}$ and $v_{h,e}$ are the reference and the estimated horizontal velocity. In the performed test, the RMSE values of position estimated by the proposed and conventional systems

https://doi.org/10.1017/S0373463318000140 Published online by Cambridge University Press

Table 3. Summary of the performance evaluation for the proposed and conventional systems in the field tests.

Distance/Time	Algorithm	Position RMSE(m)	Position Maximum Error(m)	Relative Error (%)	Velocity RMSE (Knots)	Velocity Maximum Error(Knot)
55·8 Km/4 hr	Conventional System	211	403	0·38	0·192	1
	Proposed System	223·2	406	0·4	0·214	1·3

Table 4. Comparison of the computational operations in the proposed and the conventional systems.

Algorithm	Scalar multiplication	Matrix inversion	Trigonometric functions
Conventional System	4,237	1	6
Proposed System	23	0	0

are 223 m and 211 m, respectively, and their relative values are 0·4% and 0·38%, respectively. The RMSE of velocity estimated by the proposed and conventional systems are 0·214 Knots and 0·192 Knots, respectively.

The point to be focused on here is that the superiority of the proposed system is in having a low computational load. In order to evaluate the computational complexity, the number of operations including the scalar multiplication, matrix inversion and trigonometric functions are compared in both the proposed and conventional systems. The conventional system needs 4,237 scalar multiplications, one matrix inversion and six trigonometric calculations while in the proposed system only 23 scalar multiplications are executed.

In order to compare the computational load of the algorithms, the conventional and proposed algorithms were implemented on an Intel Core2Duo CPU (E7300, 2·66GHz). It can do 2·9 Giga Floating point Operations Per Second (2·9 GFLOPS). Experimental results show that each time step of the conventional algorithm takes 0·2 ms on this CPU, while the proposed algorithm takes 0·015 ms. In other words, the conventional algorithm requires an execution time 13 times longer than that of proposed algorithm to achieve the same precision. This shows a significant decrease in the computational load.

A summary of the field results and a comparison of the number of computational operations are given in Tables 3 and 4.

5. CONCLUSION. The objective of this study was a reduction of the computational burden in a conventional underwater integrated navigation system. The conventional systems consist of a 3D INS and a 3D DVL, and in these systems, data incorporation is performed by a Kalman filter, that is by a 3D form of computations. In the proposed system, assuming only small variations of roll and pitch angles and depth being available through a pressure sensor, computations were performed in a 2D form. The nonlinear model of the system was also simplified to a linear model due to the low speed of the test vehicle. Furthermore, a low complexity KF algorithm was proposed according to the simplifications of the state covariance matrix. In order to evaluate the performance of the proposed system, a sea test was conducted. Results demonstrate that the proposed system can have a performance similar to a conventional system, while considerably reducing the computational burden.

https://doi.org/10.1017/S0373463318000140 Published online by Cambridge University Press

REFERENCES

Brandt, A. and Gardner, J.F. (1996). Constrained Navigation Algorithms for Strapdown Inertial Navigation Systems with Reduced Set of Sensors. *Proceedings of the 25th Annual Technical Symposium of the International Loran Association*, Lisbon, Portugal.

Farrell, J.A. (Ed.), 2008. *Aided Navigation, GPS with High Rate Sensors*. McGraw-Hill.

Forssell, B. (2008). *Radionavigation Systems*. Artech House.

Gao, W., Li, J., Zhou, G. and Li, Q. (2015). Adaptive Kalman Filtering with Recursive Noise Estimator for Integrated SINS/DVL Systems. *The Journal of Navigation*, **68**, 355–366.

Georgy, J., Noureldin, A., Korenberg, M.J. and Bayoumi, M.M. (2010). Low-cost three-dimensional navigation solution for RISS/GPS integration using mixture particle filter. *IEEE Transactions on Vehicular Technology*, **59**, 599–615.

Grenon, G., An, P.E., Smith, S.M. and Healy, A.J. (2001). Enhancement of the Inertial Navigation System for the Morpheus Autonomous Underwater Vehicles. *IEEE Journal of Oceanic Engineering*, **26**, 548–560.

Grewal, M.S., Weill, L.R. and Andrews, A.P. (2007). *Global Positioning System, Inertial Navigation, and Integration.* John Wiley and Sons, Inc.

Hegrenaes, O. and Hallingstad, O. (2011). Model-aided INS with Sea Current Estimation for Robust Underwater Navigation. *IEEE Journal of Oceanic Engineering*, **36**, 316–337.

Hoshizaki, T. and Tashiro, E. (2009). Computational Scheme for MEMS Inertial Navigation Systems. Patent Application Publication.

Iqbal, U., Karamat, T.B., Okou, A.F. and Noureldin, A. (2009). Experimental results on an integrated GPS and multisensor system for land vehicle positioning. *International Journal of Navigation and Observation*, **2009**, 1–18.

Iqbal, U., Okou, A.F. and Noureldin, A. (2008). An Integrated Reduced Inertial Sensor System-RISS / GPS for Land Vehicle. *IEEE Proceedings of IEEE/ION PLANS*, Monterey, CA.

Kaygisiz, B.H. and Sen, B. (2015). In-motion Alignment of a Low-cost GPS/INS under Large Heading Error. *The Journal of Navigation*, **68**, 355–366.

Kinsey, J.C., Eustice, R.M. and Whitcomb, L.L. (2006). A survey of Underwater Vehicle Navigation: Recent Advances and New Challenges. *IFAC Conference Manoeuvre Control Marine Craft*, Lisbon, Portugal.

Lee, P.M., Jun, B.H., Kim, K., Lee, J., Aoki, T. and Hyakudome, T. (2007). Simulation of an Inertial Acoustic Navigation System with Range Aiding for an Autonomous Underwater Vehicle. *IEEE Journal of Oceanic Engineering*, **32**, 327–345.

Maybeck, P.S. (1979). *Stochastic Models, Estimation, and Control.* Academic Press.

McEwen, R., Thomas, H., Weber, D. and Psota, F. (2005). Performance of an AUV Navigation System at Arctic Latitudes. *IEEE Journal of Oceanic Engineering*, **30**, 443–454.

Miller, P.A., Farrell, J.A., Zhao, Y. and Djapic, V. (2010). Autonomous Underwater Vehicle Navigation. *IEEE Journal of Oceanic Engineering*, **35**, 663–678.

Sarkka, S. (2013). *Bayesian Filtering and Smoothing.* Cambridge University Press.

Shabani, M. and Gholami, A. (2016). Improved Underwater Integrated Navigation System using Unscented Filtering Approach. *The Journal of Navigation*, **69**, 561–581.

Shabani, M., Gholami, A. and Davari, N. (2015). Asynchronous Direct Kalman Filtering Approach for Underwater Integrated Navigation System. *Nonlinear Dynamics*, **80**, 71–85.

Shabani, M., Gholami, A., Davari, N. and Emami, M. (2013). Implementation and Performance Comparison of Indirect Kalman Filtering Approaches for AUV Integrated Navigation System using Low Cost IMU. *ICEE2013*, Mashhad, Iran, 1–6.

Simon, D. (2006). *Optimal State Estimation: Kalman, H-infinity, and Nonlinear Approaches*. John Wiley & Sons.

Titterton, D.H. and Weston, J.L. (2004). *Strapdown Inertial Navigation Technology*. The Institution of Electrical Engineers, Inc.

Valade, A., Acco, P., Grabolosa, P. and Fourniols, J.Y., (2017). A Study about Kalman Filters Applied to Embedded Sensors. *MDPI Sensors*, **17**, 2810–2822.

Vasilijevic, A., Borovic, B. and Vukic, Z. (2012). Underwater Vehicle Localization with Complementary Filter: Performance Analysis in the Shallow Water Environment. *Journal of Intelligent and Robotic System*, **68**, 373–386.

Wang, Q., Li, Y. and Niu, X. (2016). Thermal Calibration Procedure and Thermal Characterization of Low-cost Inertial Measurement Units. *The Journal of Navigation*, **69**, 373–390.

Xian, Z., Hu, X. and Lian, J. (2014). Fusing Stereo Camera and Low-Cost Inertial Measurement Unit for Autonomous Navigation in a Tightly-Coupled Approach. *The Journal of Navigation*, **68**, 737–452.

Yun, X., Bachmann, E.R., McGhee, R.B., Whalen, R.H., Roberts, R.L., Knapp, R.G., Healey, A.J. and Zyda, M.J. (1999). Testing and Evaluation of an Integrated GPS/INS System for Small AUV Navigation. *IEEE Journal of Oceanic Engineering*, **24**, 396–404.

Zhang, Q., Niu, X., Zhang, H. and Shi, C. (2013). Algorithm Improvement of the Low-end GNSS/INS Systems for Land Vehicles Navigation. *Mathematical Problems in Engineering*, **2013**, 1–12.

https://doi.org/10.1017/S0373463318000140 Published online by Cambridge University Press